Immunostimulatory Effects of Silver Nanoparticles in Immune Cells and their Relevance to Atopic Dermatitis

SeungJae Kim

The Graduate School
Yonsei University
Graduate Program for Nanomedical Science

Immunostimulatory Effects of Silver Nanoparticles in Immune Cells and their Relevance to Atopic Dermatitis

Directed by Professor In-Hong Choi

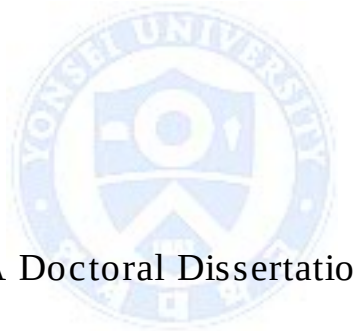

A Doctoral Dissertation

Submitted to Graduate Program for Nanomedical Science

and the Graduate School of Yonsei University

in partial fulfillment of the requirements for the degree of

Doctor of Philosophy

SeungJae Kim

August 2015

This certifies that the Doctoral Dissertation of

SeungJae Kim is approved.

_____

Thesis Supervisor : In-Hong Choi

_____

Thesis Committee Member : Jeon-Soo Shin

_____

Thesis Committee Member : Kangtaek Lee

_____

Thesis Committee Member : Donghyun Kim

_____

Thesis Committee Member : Il-Je Yu

The Graduate School Yonsei University

August 2015

감사의 글

먼저 부족한 저에게 많은 기회를 주시고 지도해 주신 최인홍 교수님께 말로는 다 할 수 없는 감사 드립니다. 아무것도 몰랐던 저에게 나노라는 새로운 길을 가르쳐 주시고, 항상 보듬어 주시고, 격려해 주셨기에 여기까지 올 수 있었던 것 같습니다. 지도교수님 이상으로서 어머니처럼 6년간 저를 이끌어 주심을 잊지 않도록 하겠습니다. 언제나 미생물학교실 주임 교수님으로서, 이번에는 심사위원으로서 마지막까지 도움을 주신 신전수 교수님께 감사의 말씀 드립니다. 항상 나노 물질 합성에 도움을 주셨고, 이번에도 논문 지도를 맡아주신 이강택 교수님께 감사를 드립니다. 또한 언제나 따뜻한 관심으로 논문 지도를 해주신 김동현 교수님과 유일제 교수님께 감사의 말씀 드립니다. 제가 생활하던 미생물학교실의 조상래 교수님, 박전한 교수님, 김종선 교수님, 이재면 교수님, 윤상선 교수님, 유제욱 교수님, 신성재 교수님, 나노메디컬 협동과정의 유경화 교수님, 실험에 도움을 주셨던 이광훈 교수님, 박승우 교수님, 김세훈 교수님 많은 교수님들의 도움으로 학위를 마무리 할 수 있었습니다. 감사합니다.

지금은 질병관리본부에 계시지만 대학원 생활 중 항상 곁에서 격려와 응원을 해주신 양은정 박사님, 언제나 든든한 형처럼 옆을 지켜준 진원형, 어리버리한 후배 잘 이끌어주신 든든한 사수 지영샘, 마지막까지 함께해준 유일한 후임 한구 덕분에 실험실 생활이 즐거웠던 것 같습니다. 짧은 시간이었지만 많은 도움 주신 장영생 박사님께도 감사 드립니다. 또한 항상 나노 물질 합성에 도움을 주셨던 강태경 선생님, 아토피 연구에 도움을 주신 김산 선생님 감사합니다.

또한 대학원 생활 중에 언제나 도움을 주신 고시환 선생님, 최영미 선생님, 곽만섭 박사님, 오영택 박사님, 김주영 박사님 감사합니다. 나노메디컬 협동과정으로서 항상 듬직하게 도움을 준 영욱이형, 희열이형, 현국형 감사합니다. 지금은 졸업하였지만 지유, 정현, 형준이 덕분에 많은 도움을 받았습니다. 나노메디컬 동기들 중 이제 제가 마지막으로 졸업을 하게 되었네요. 모두 고생하셨고 감사합니다.

실험실 생활 중 유일한 동갑이었던 몸짱 효준이, 형 같은 동생 욱진이, 왈가닥 아가씨 유리, 항상 침착한 어른아이 의덩이, 항상 파이팅 넘치는 야롱이, 웃음과 애교담당 한슬이, 바쁜데도 항상 묵묵히 나와 같은 길을 함께해준 경배, 이젠 아기 아빠가 되어 나보다 어른이 되어버린 준혁이, 캐나다인으로 제 2의 인생을 시작한 바리, 대학원생의 모범의 모습을 보여주는 상준이, 수정샘, 미생물학 교실 최강미남 창모, 용근이 덕분에 잊지 못할 정도로 많은 추억을 쌓게 되었습니다. 이후에도 항상 도움이 되는 사람이 되기 위해 노력하겠습니다.

이젠 어느새 20년이 되어버린 내 삶의 반떵이들 수한, 정봉, 형식, 광현, 선숙, 화영, 승민, 성환이 10년은 함께해온 위니누나, 레이나누나, 폴형, 현모형, 소리 덕분에 항상 버틸 수 있었던 것 같습니다.

마지막으로 지금까지 제가 있을 수 있게 해주신 부모님, 누나, 매형까지 항상 칭얼대고, 투정만 부렸는데 어느새 이렇게 졸업까지 하게 되었네요. 말은 항상 더 잘하겠다고 하지만, 항상 최선을 다해 살도록 노력하겠습니다. 감사합니다.

이하 모든 분들에게 감사 드리며 김승재 드림.

CONTENTS

LIST OF FIGURES

I. Effects of silver nanoparticles in mast cells and an atopic mouse model

II. Effects of silver nanoparticles in macrophages

ABSTRACT

Immunostimulatory Effects of Silver Nanoparticles in Immune Cells and their Relevance to Atopic Dermatitis

SeungJae Kim

Graduate Program for Nanomedical Science

The Graduate School Yonsei University

(Directed by Professor In-Hong Choi)

Engineered nanomaterials (NMs) are increasingly used in numerous consumer products and biomedical applications that affect humans directly and indirectly. However, in vitro and in vivo studies have revealed that nanomaterials can result in toxicity. The immunostimulatory effect of silver nanoparticles (AgNPs) is dependent on particle size and the production of reactive oxygen species (ROS). Although these products have many opportunities to contact with the skin, the toxicity of AgNPs has not been clearly defined.

Mast cells are potent effectors of the allergic response. They play an important role in asthma, atopic dermatitis (AD) and other allergic reactions. In this study, RBL2H3 mast cell viability was dependent on the particles size. Granule release, Ca^{2+}

influx, the production of hydrogen peroxide and superoxide and mitochondrial membrane damage were used to evaluate cytotoxicity of AgNPs. To evaluate the synergistic effect of AgNPs on the induction of allergic reactions in animals, NC/Nga mice were used in this study. NC/Nga mice spontaneously develop an eczematous AD-like skin lesion when kept under conventional conditions, but not when maintained under specific pathogen-free (SPF) conditions. They are considered an appropriate animal model for AD.

Macrophages are active phagocytic cells present in many tissues. The internalization of nanoparticles by phagocytic cells can occur through phagocytosis/macropinocytosis, receptor-mediated endocytosis and passive penetration. Phagocytosis and macropinocytosis are mediated by actin polymerization, which causes cell membrane ruffling. The process is inhibited by cytochalasin D. Endocytosis can occur as clathrin-dependent endocytosis and caveolae-dependent endocytosis. Clathrin-dependent endocytosis is inhibited by chlorpromazine, a cationic amphiphilic drug that prevents the recycling of clathrin. Caveolae-dependent endocytosis is inhibited by nystatin, an antibiotic and sterol-binding agent that removes membrane cholesterol, which is important for maintaining and sealing the membrane of caveolae.

In this study, the ability of AgNPs to evoke allergic immune responses was investigated in mast cells and macrophages (in vitro) and atopic animal model (in vivo) to assess. Cytotoxicity in mast cells was evaluated using Cell Counting Kit-8 (CCK8). Cell death was induced by 5 nm AgNPs, but not by 100 nm AgNPs. Granule release was evaluated with the β-hexosaminidase assay. Granule release in RBL2H3 cells was induced by 5 nm AgNPs, but not by 100 nm AgNPs. N-acetylcystein (NAC) at 5 mM

inhibited granule release in RBL2H3 cells. To assess intracellular Ca^{2+} levels, RBL2H3 cells were prestained with Fluo4-AM and then treated with AgNPs in HBSS with and without Ca^{2+}. In both groups with and without Ca^{2+}, 5 nm AgNPs but not 100 nm AgNPs increased the fluorescence intensity. To evaluate the effect of intracellular Ca^{2+} levels on granule release, RBL2H3 cells were pretreated with thapsigargin and then treated with AgNPs. Thapsigargin inhibited the granule release induced by 5 nm AgNPs. In addition, the production of hydrogen peroxide and superoxide was assessed by staining RBL2H3 cells with CM-H_2DCFDA or MitoSOX, respectively. Treatment with 5 nm AgNPs increased the fluorescence intensity of CM-H_2DCFDA and MitoSOX in a dose-dependent manner. In addition, JC-1 staining was performed to assess mitochondrial depolarization. JC-1 fluorescence intensity decreased in cells treated with 5 nm AgNPs. To investigate the synergistic effect of AgNPs on the induction of AD, ear thickness was measured once a week and the severity score of the AD-like skin lesions was evaluated once a week. Ear swelling was more severe in mice treated with 5 nm AgNPs + Ad Biostir when compared with that in the AD control group. The severity score of the skin also increased in mice treated with 5 nm AgNPs. Epidermal thickness in the group treated with 5 nm AgNPs + Ad Biostir was thicker when compared to that of the Ad Biostir-only group. The number of infiltrated mast cells in skin lesions was higher in the group treated with 5 nm AgNPs + Ad Biostir than in the Ad Biostir-only group. Total IgE levels in the serum increased in the group treated with 5 nm AgNPs + Ad Biostir.

The viability of U937 cells declined abruptly when cells were treated with 5 nm AgNPs. The effects of AgNP endocytosis or phagocytosis on cell death were then evaluated. After treatment of U937 cells with AgNPs, neither chlorpromazine,

cytochalasin D, nor nystatin prevented cell death. At relatively high concentrations, chlorpromazine, cytochalasin D and nystatin partially inhibited the production of IL-8 following exposure to AgNPs. These findings were confirmed with real-time RT-PCR assays.

Collectively, it was suggested that these immunostimulatory effects has contributed to causing AD. These inflammatory effects should be considered and evaluated in addition to cytotoxicity when studying the effects of AgNPs exposure in human physiology.

Keywords: Silver nanoparticles, Mast cells, Macrophages, ROS, Ca^{2+}, Cytotoxicity, Allergy

ABBREVIATIONS

AD	Atopic dermatitis
AgNPs	Silver nanoparticles
CCK8	Cell counting kit-8
cDNA	Complementary DNA
DLS	Dynamic light scattering
DNA	Deoxyribose nucleic acid
ELISA	Enzyme-linked immunosorbent assay
ER	Endoplasmic reticulum
FBS	Fetal bovine serum
HBSS	Hank's balanced salt solution
HDM	House dust mite
H&E	Hematoxylin and eosin
IL	Interleukin
IgE	Immunoglobulin E
LTs	Leukotrienes
MEM	Minimum essential medium
NAC	N-acetyl-1-cysteine
NMs	Engineered nanomaterials
OD	Optical density
PBS	Phosphate buffered saline
PGD2	Prostaglandin D2
p-NAG	P-nitrophenyl N-acetyl-β-D-glucosamide
PVP	Polyvinylpyrrolidone
RBL2H3 cell	Rat basophilic leukemia cell line
RNA	Ribonucleic acid
ROS	Reactive oxygen species
RT-PCR	Real-time reverse transcription polymerase chain reaction
SDS	Sodium dodecyl sulfate
SPF	Specific pathogen-free
TEM	Transmission electron microscopy

I. Effects of silver nanoparticles in mast cells and an atopic mouse model

1. Introduction

Engineered nanomaterials (NMs) are increasingly used in consumer products and biomedical applications that affect to humans directly and indirectly (1-5). However, *in vitro* and *in vivo* studies have revealed that NMs can result in toxicity. When individuals are exposed to nanoparticles, the nanoparticles translocate from the entry site into the blood and enter the systemic circulation (6), where they are detected and internalized by macrophages or monocytes (7, 8). The physical and chemical properties (e.g., size, shape, surface chemistry, composition and aggregation) of NMs are known to induce toxic effects. Silver nanoparticles (AgNPs) induce significant toxicity in NMs (4). The immunostimulatory effect of AgNPs depends on particle size and the production of reactive oxygen species (ROS) (9). The antibacterial activity of AgNPs, has been employed in many products (e.g., wound dressings, biofilms and dental carriers) (10). Although these products have many opportunities to contact the skin, the toxicity of AgNPs has not been clearly defined.

Mast cells are potent effectors of the allergic response. They play an important role in asthma, atopic dermatitis (AD) and other allergic reactions. MC activation occurs through the cross-linking of an antigen with two IgE molecules bound to FcεRI, leading to the release of mediators. These mediators induce allergic skin inflammation (11). Upon stimulation, mast cells release a variety of preformed and newly

synthesized inflammatory mediators, including histamine, IL-4, IL-5, IL-6 and tumor necrosis factor-α (TNF- α). In addition, proteinases (tryptase, chymase and carboxypeptidase) and newly generated lipid mediators such as prostaglandin (PGD2), leukotrienes (LTs) and platelet-activating factor are released (12). The binding of IP3 to specific receptors in the endoplasmic reticulum (ER) results in the depletion of Ca^{2+} stores, which activates store-operated Ca^{2+} entry from the extracellular medium. Btk, SLP-76, LAT and PLC-γ are essential for generating signals for sustained Ca^{2+} influx. Ca^{2+} influx leads to granules exocytosis and the generation of LTs and cytokines (13). The activated mast cells release chemical mediators, such as histamine, LTs and PGD2. These mediators lead to immediate phase reactions in the tissue, such as redness and itching, shortly after allergen-IgE binding. In the later phases of the disease, IL-4 and IL-13 are generated and released several hours after allergen-antibody cross-linking (14).

AD is a common chronic or chronically relapsing, noncontagious and pruritic inflammatory skin disorder (15). AD has various causes, including the abnormal activation of immunological and inflammatory pathways resulting in a defective skin barrier, exposure to environmental agents and neuropsychological factors (16, 17, 18). Approximately 70%-80% of AD patients present with the “extrinsic” form of AD. They have elevated serum IgE levels and IgE antibodies to environmental and/or food allergens. The remaining 20%–30% present with the “intrinsic” form of AD, with low serum IgE levels and no evidence of IgE antibodies (19). The clinical features of AD include erythema, edema, vesiculation, crusting, dryness, scaling, excoriations and lichenification. Itching is a chief symptom and can be very troublesome (20).

To evaluate the synergistic effect of AgNPs on the induction of allergic reactions in animals, NC/Nga mice were used in this study. The NC/Nga mice were generated from Japanese fancy mice and were established as an inbred strain in 1957 (21). NC/Nga mice spontaneously develop an eczematous AD-like skin lesion when kept under conventional conditions, but not when maintained under specific pathogen-free (SPF) conditions. They are considered an appropriate animal model for AD (22).

In this study, the activation of mast cells by silver nanoparticles was investigated in mast cells (*in vitro*) and atopic animal models (*in vivo*) to assess the ability of AgNPs to evoking allergic immune responses. The results of this study increase our understanding of the immunostimulatory effect of AgNPs, particularly in allergic diseases.

2. Materials and Methods

2.1. AgNPs

AgNPs in an aqueous suspension were provided by I&C (5 nm; Seoul, Korea) or purchased from ABC Nanotech (100 nm; Daejeon, Korea). Briefly, AgNPs (5 nm and 100 nm) were synthesized by the reduction of $Ag(NO_3)$. All AgNPs were round and polyvinylpyrrolidone (PVP)-coated. Endotoxin contamination tests using the PyroGene recombinant factor C assay (Cambrex Bioscience, Walkersville, MD, USA.) were negative (endotoxin <0.01 U/mL). For cell culture, different concentrations of AgNPs were prepared in minimum essential medium (MEM) with 2 mM L-glutamine supplemented with 10% fetal bovine serum (FBS), 100 U/mL penicillin and 100 U/mL streptomycin.

2.2. Characterization of AgNPs

The diameter was determined with transmission electron microscopy (TEM, model JEM-1011, JEOL, Tokyo, Japan). Agglomeration of the nanoparticles in MEM with 10% FBS at 1, 5 and 15 μg/mL was analyzed using dynamic light scattering (DLS) (Malvern Instruments, Novato, CA, USA.).

2.3. Cell culture

The RBL2H3 rat mast cells (ATCC, Manassas, VA, USA.) were cultured in MEM containing 10% FBS at 37℃ in a moisturized 5% CO_2 incubator. Although endotoxin was not detected in the AgNPs used in this study, polymyxin B (InvivoGen, San Diego,

CA, USA.) at a concentration of 10 ng/mL was added as an endotoxin neutralizer. The culture medium was changed every 2-3 days to maintain a cell density of approximately 2×10^6 cells/mL.

2.4. Cytotoxicity assay

Cell viability was assessed using the Colorimetric Cell counting Kit-8 (CCK-8) (Dojindo Laboratories, Kyoto, Japan). CCK-8 is a colorimetric assay that uses a highly water-soluble tetrazolium salt, WST-8[2-(2-methoxy-4-nitrophenyl)-3-(4-nitrophenyl)-5-(2,4-disulfophenyl)-^{2}H-tetrazolium, monosodium salt]. Cells were plated in 24-well plates at 4×10^5 cells in 500 μL of MEM supplemented with 10% FBS and incubated overnight in a 5% CO_2 incubator. The medium was then removed and the cells were washed twice with Hank's balanced salt solution (HBSS). The cells were then treated with 400 μL/mL of AgNP solution diluted in MEM supplemented with 10% FBS. After 24 hr, 15 μL of CCK-8 reagent was added to each well and incubated at 37℃ for 2 hr. After centrifugation, 100 μL of supernatant was transferred to 96-well microtiter plates and the optical density (OD) was measured at 450 nm. As pretreatment, NAC (SigmaeAldrich, St. Louis, MO, USA) at 5-10 mM was added for 30 min before the treatment with AgNPs.

2.5. Granule release assay

Cells were plated at a density 4×10^5 cells in 24-well plates in 500 μL of MEM supplemented with 10% FBS and incubated in a 5% CO_2 incubator. After overnight incubation, the medium was removed and the cells were washed with HBSS. The cells were then treated with 200 μL of AgNP solution diluted in HBSS. β-Hexosaminidase

release from RBL2H3 cells was measured by incubating 25 μL of the supernatant or lysed cell pellet with 5% Triton X-100 in 25 μL of p-nitrophenyl N-acetyl-β-D-glucosamide (p-NAG) in a 96-well plate (Nunc, Roskilde, Denmark) for 2 hr at 37°C. The reaction was stopped by the addition 250 μL of 0.2 M glycine (pH = 10.6) and the OD was read at 405 nm.

2.6. Assay for total ROS and mitochondrial superoxide

After treatment with AgNPs for 30 min, cells in HBSS were stained with 2 μM CM-H_2DCFA (Invitrogen, Carlsbad, CA, USA) for 30 min to detect reactive hydrogen peroxide and 2 μM MitoSOX (Invitrogen) for 15 min to detect mitochondrial superoxide. Staining was performed at 37°C in the dark. Cells were stained with 2 μM of JC-1 (Invitrogen) to assess mitochondrial depolarization. The OD was detected using a VICTOR X4 multi label plate reader (Perkin-Elmer, Norwalk, CT, USA.) at 580 nm for CM-H_2DCFA or 510 nm for MitoSOX.

2.7. Assay for mitochondrial membrane integrity

After treatment with AgNPs for 30 min, cells were stained with 2 μM of JC-1 (Invitrogen) for 15 min at 37°C in the dark. The OD was read at 590 nm using a VICTOR X4 multi label plate reader (Perkin-Elmer).

2.8. Ca^{2+} influx assay

Cells were stained with Fluo4-AM (Invitrogen) for 30 min and diluted in HBSS at 37℃ in the dark. After treatment with fluorescent dyes, Cells were treated with AgNPs. After treatment with nanoparticles, cells were monitored using a Victor X4 multi label plate reader (Perkin-Elmer) at a constant temperature of 36℃ and measured every 5 sec for 600 sec.

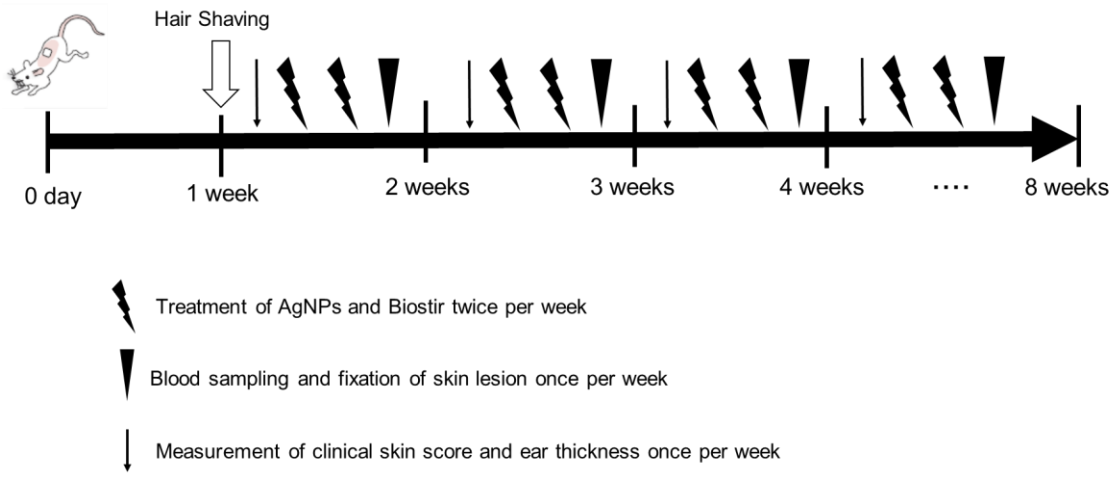

2.9. Atopic animal model and induction of AD

Six-week-old female NC/Nga mice weighing 22 ± 2 g were purchased from Central Lab. Animal Inc. (Seoul, Korea) and maintained for 1 week before experiments. All animal experiments were performed in compliance with the guidelines of Yonsei University Institutional Animal Care and protocols were reviewed and approved by the Institutional Animal Care and Use Committees of the Laboratory Animal Research Center at Yonsei University Health System (Permit Number: 2013-0176-2). All mice were maintained in the SPF facility of the Yonsei Laboratory Animal Research Center.

To induce AD, the hair on the back was shaved with depilatory cream (Veet, Oxy Reckitt Benckiser Ltd. Slough, USA) 1 day before experiments. For barrier disruption, 150 μL of 4% (w/v) sodium dodecyl sulfate (SDS) was applied to the shaved dorsal skin and ear skin. After 2 hr, 100 μL of AgNPs was added to the same regions and left for 2 hr. Thereafter 100 mg of Ad Biostir (Biostir, Kobe, Japan) was applied. Ad Biostir prepared from house dust mites, a crude extract allergen of Dermatophagoides farina (21). The skin treatment was performed twice a week for 8

weeks. The mice (n = 12) were allocated to four groups (3 mice/group): Ad Biostir-only group (100 μL distilled water + Ad Biostir), 5 nm AgNP 40 μg/mL group (100 μL of 5 nm AgNPs at 40 μg/mL + Ad Biostir), 5 nm AgNP 400 μg/mL group (100 μL of 5 nm AgNPs at 400 μg/mL + Biostir-AD) and 5 nm AgNP 4,000 μg/mL group (100 μL of 5 nm AgNPs at 4,000μg/mL + Ad Biostir).

2.10. Measurement of clinical skin score

The clinical skin score is the sum of individual scores graded as 0 (absence), 1 (mild), 2 (moderate) and 3 (severe) for each of four signs and symptoms (erythema/hemorrhage, scaling/dryness, edema and excoriation/erosion).

2.11. Histopathological analysis

AD-like skin lesions were selected and 2 mm punch biopsies were performed for immunohistochemistry. Skin lesions were fixed with 10% neutral formalin, embedded in paraffin and sectioned to a depth of 10 μm. To detect the epidermal thickness and infiltration of inflammatory cells, sections were stained with hematoxylin–eosin (H&E). Toluidine blue staining was performed to count the number of mast cells. All stained sections were observed under a microscope with twin CCD cameras (magnification, ×100, ×400; Olympus, Tokyo, Japan).

2.12. Detection of total IgE in the serum

Blood samples (100 μL) were collected from the retro orbital plexus every week and the serum was separated by centrifugation at 2,000 rpm for 5 min and stored at -20°C until use. The serum IgE levels were analyzed using the mouse IgE ELISA kit (432402; Biolegend, San Diego, CA, USA.). The microplates (Nalgen; Nunc International, Naperville, IL, USA) were coated with coating buffer and IgE capture antibody overnight at 4°C and then blocked with 10% FBS in phosphate-buffered saline (PBS) for 1 hr at room temperature. Serially diluted serum samples (1:100-1:1,000) were added and incubated for 2 hr at room temperature. The plates were then washed with PBS plus 0.05% Tween 20, Incubated for 2 hr with horseradish peroxidase–conjugated rat anti-mouse IgE antibodies and washed with again PBS plus 0.05% Tween 20. The color reaction was developed with 3, 3′, 5, 5′-tetramethylbenzidine and stopped with 1 N H_2SO_4. The absorbance was read at 450 nm with a microplate reader. IgE levels were determined by comparing the OD values of the study groups to the OD values of standard IgE.

2.13. Statistical analysis

Data were expressed as the mean ± SD. The statistical comparisons were performed using Student's t-test for two groups and ANOVA with Bonferroni post-tests for more than two groups. Statistical analyses were performed using GraphPad Prism 5. A p-value of less than 0.05 was considered significant.

3. Results

3.1. Characterization of AgNPs

In TEM images, the AgNPs (5 nm and 100 nm) were relatively uniform in size (Fig. 1A). DLS analysis by number showed that the mean size was 5.1 nm for the 5 nm AgNPs and 74.2 nm for the 100 nm particles (Fig. 1B).

(A) TEM analysis

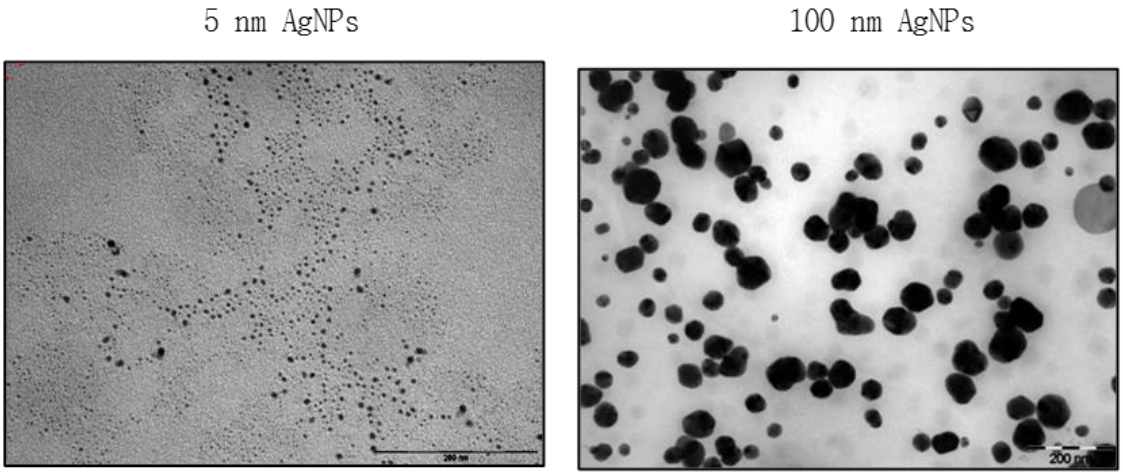

(B) DLS diameter

5 nm AgNPs	100 nm AgNPs
Intensity : 6.6 nm (35.5%)	Intensity : 132.6 nm (100%)
Volume : 4.2 nm (99%)	Volume : 111.1 nm (100%)
Number : 5.1 nm (100%)	Number : 74.2 nm (100%)

Figure 1. Characterization of AgNPs. (A) TEM images of AgNPs showed that the 5 nm and 100 nm particles were relatively uniform in size. (B) DLS analysis by number showed that the mean size was 5.1 nm for the 5 nm AgNPs and 74.2 nm for the 100 nm AgNPs. For DLS analysis. AgNPs were dispersed in MEM containing 10% FBS.

3.2. Cytotoxicity in mast cells

As shown in Fig. 2, cell death was induced by 5 nm AgNPs starting at 1.2 μg/mL, but not by 100 nm AgNPs. The LC_{50} of the 5 nm AgNPs was 1.96 μg/mL. Cell death was not induced by 100 nm AgNPs at concentrations up to 4 μg/mL. Therefore, cytotoxicity was dependent on the particle size. Cell death was completely inhibited by NAC at 5 mM.

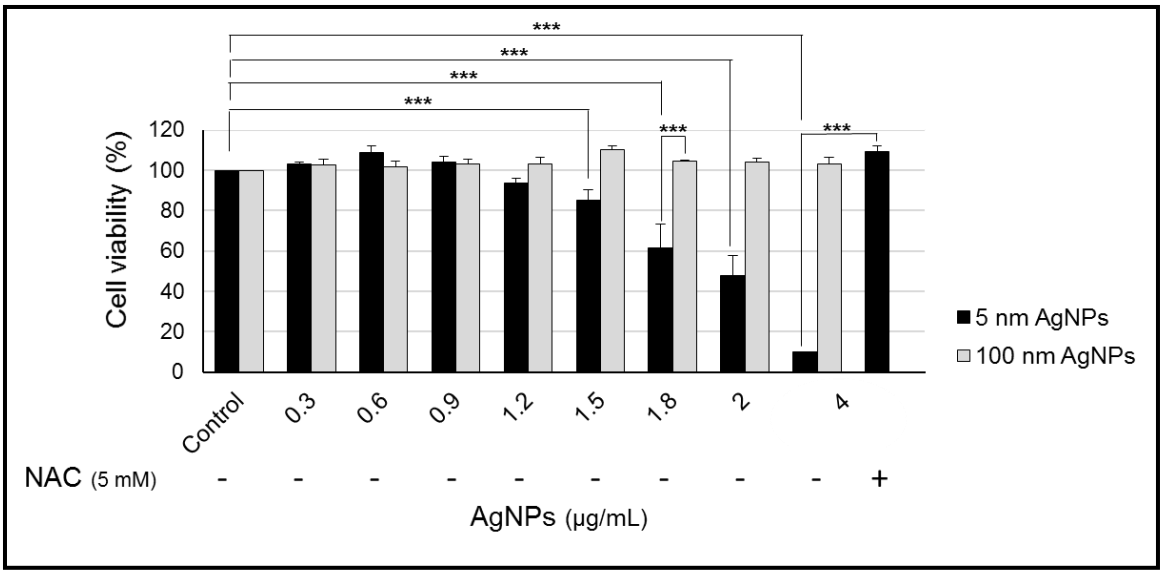

Figure 2. Cytotoxicity of AgNPs in mast cells. RBL2H3 cells were treated with 5 nm or 100 nm AgNPs for 24 hr, and cytotoxicity was determined with the CCK-8 assay. Cells were treated with NAC for 30 min before treatment with AgNPs. The LC_{50} of the 5 nm AgNPs was approximately 1.96 μg/mL. Data represent the mean ± SD. ***p < 0.001.

3.3. Granule release in mast cells

Granule release of 18.9%-76.9% in RBL2H3 cells was induced by 0.15 μg/mL-0.6 μg/mL of 5 nm AgNPs, but not by 100 nm AgNPs. Phorbol 12-myristate 13-acetate (PMA)/ionomycin was used as a positive control of to induce granule release (Fig. 3A). Granule release in RBL2H3 cells was inhibited by NAC at 5 mM (Fig. 3B).

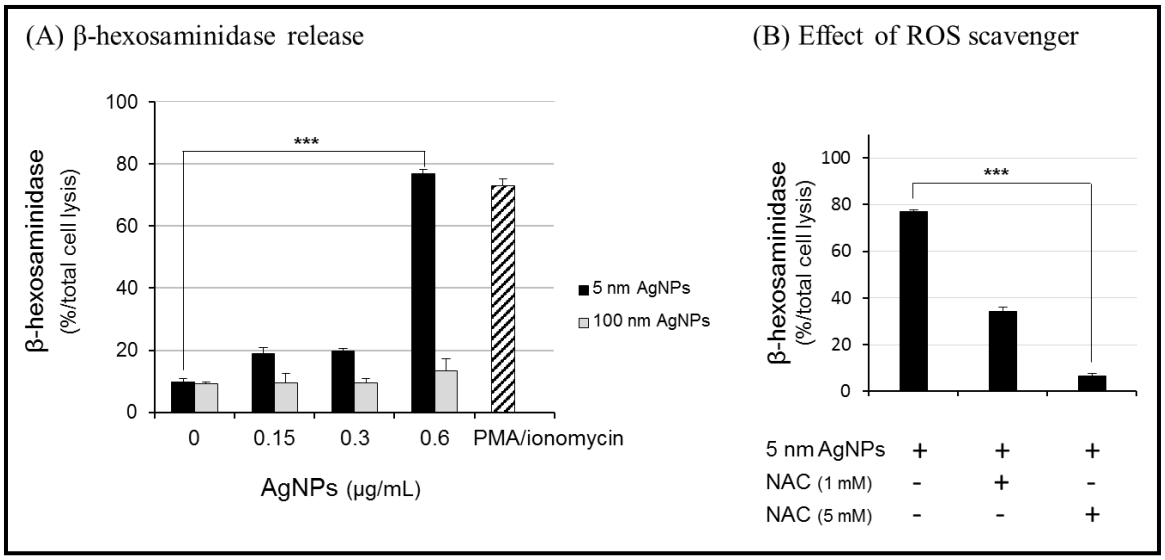

Figure 3. Granule release by AgNPs in mast cells. (A) RBL2H3 cells were treated with 5 nm AgNPs for 30 min, and granule release was determined with the β-hexosaminidase assay. (B) Cells were treated with NAC for 30 min before treatment with AgNPs. Data represent the mean ± SD. ***$p < 0.001$.

3.4. Calcium influx in mast cells and inhibition by thapsigargin

To assess intracellular Ca^{2+} levels, RBL2H3 cells were pre-stained with Fluo4-AM and then treated with AgNPs in HBSS with Ca^{2+} (Fig. 4A) or HBSS without Ca^{2+} (Fig. 4B). Treatment with 5 nm AgNPs at 2 μg/mL increased the fluorescence intensity in both groups with Ca^{2+}, 0.65-fold at 600 sec), without Ca^{2+}, 0.53-fold at 600 sec). Treatment with 100 nm AgNPs had no effect.

To evaluate the effect of intracellular Ca^{2+} levels on granule release, RBL2H3 cells were pretreated with thapsigargin and then treated with AgNPs. Thapsigargin was used to deplete the intracellular Ca^{2+} stores. Granule release induced by 5 nm AgNPs deceased from 75% without thapsigargin to 37% with thapsigargin.

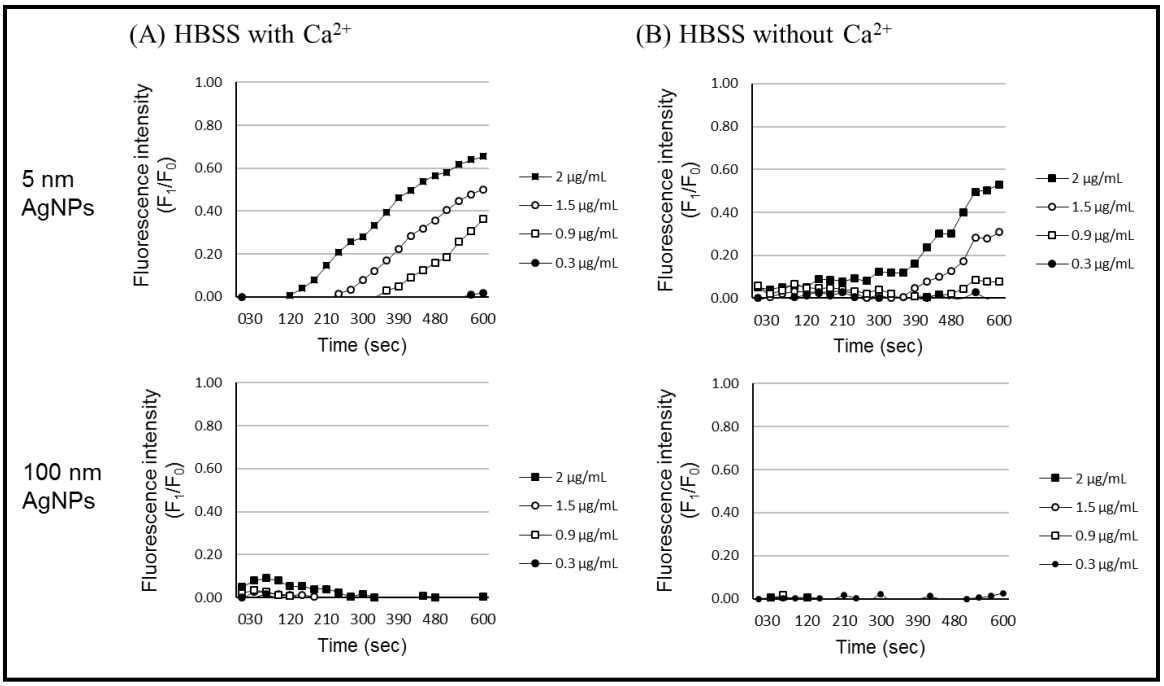

Figure 4. Detection of intracellular Ca^{2+} levels. RBL2H3 cells were pre-stained with Fluo4-AM for 30 min and then treated with AgNPs. Cells were monitored using a Victor X4 multi label plate reader and measured every 5 sec. (A) HBSS with Ca^{2+}, (B) HBSS without Ca^{2+}.

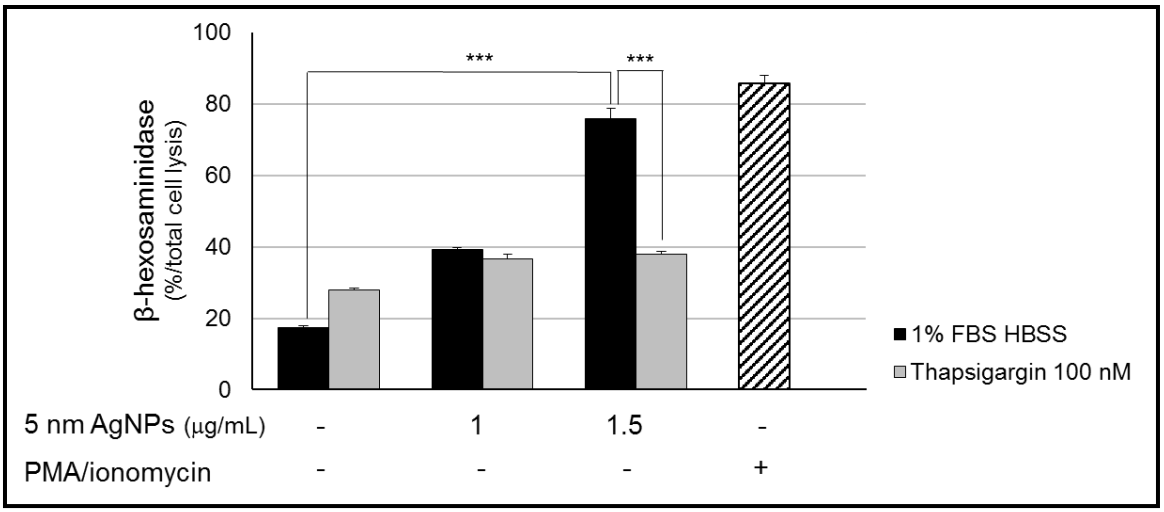

Figure 5. Inhibition of granule release by thapsigargin. RBL2H3 cells were pre-treated with thapsigargin for 30 min and then treated with 5 nm AgNPs. Granule release was determined using the β-hexosaminidase assay. Data represent the mean ± SD. ***p < 0.001.

3.5. Generation of total ROS and mitochondrial superoxide in mast cells

As shown in Fig. 6, the production of hydrogen peroxide and superoxide was assessed by staining RBL2H3 cells with CM-H2DCFDA and MitoSOX, respectively. Treatment with 5 nm AgNPs increased the production of total ROS, including hydrogen peroxide and superoxide, in a dose-dependent manner. Treatment with 4 μg/mL AgNPs increased ROS production 4.9-fold when compared with control (Fig. 6A). Mitochondrial superoxide also increased in a dose-dependent manner after 5 nm AgNPs treatment with 4 μg/mL AgNPs increased superoxide levels 2-fold when compared with control (Fig. 6B). Total ROS and mitochondrial superoxide were not affected by treatment with 100 nm AgNPs.

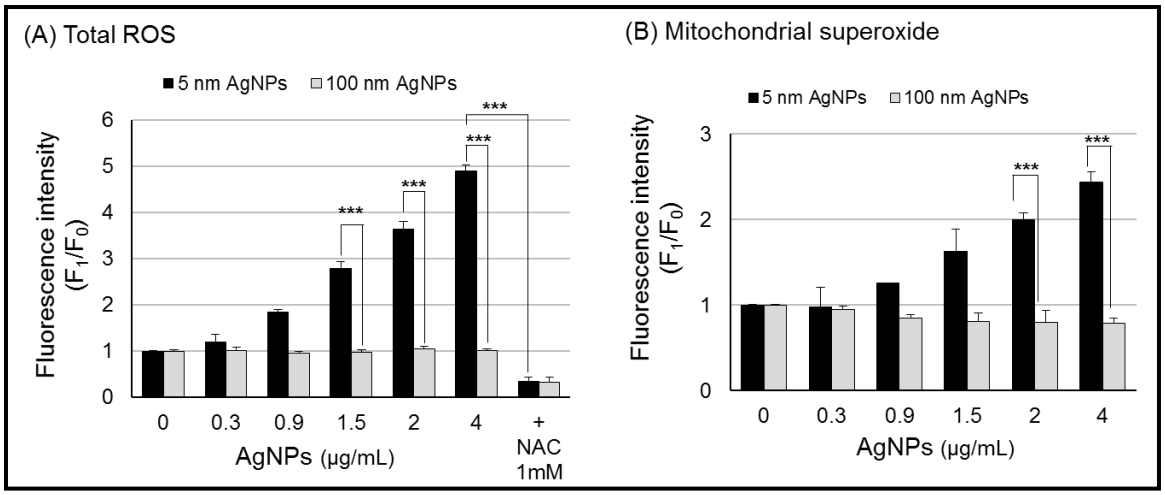

Figure 6. Generation of total ROS and mitochondrial superoxide. RBL2H3 cells were treated with AgNPs for 30 min. (A) Cells were stained with CM-H_2DCFDA for 30 min. (B) Cells were stained with MitoSOX for 15 min. The fluorescence intensity was analyzed using a Victor X4 multi label plate reader. Data represent the mean ± SD. ***$p < 0.001$.

3.6. Assessment of mitochondrial membrane integrity

Mitochondrial membrane integrity was assessed by staining cells with JC-1, a lipophilic cation used to measure mitochondrial membrane potential. The JC-1 fluorescence intensity increased 4.1-fold over that in control cells when cells were treated with 5 nm AgNPs at 4 μg/mL. The effect was dose-dependent. However, 100 nm AgNPs at concentrations up to 4 μg/mL did not increase the JC-1 fluorescence intensity (Fig. 7).

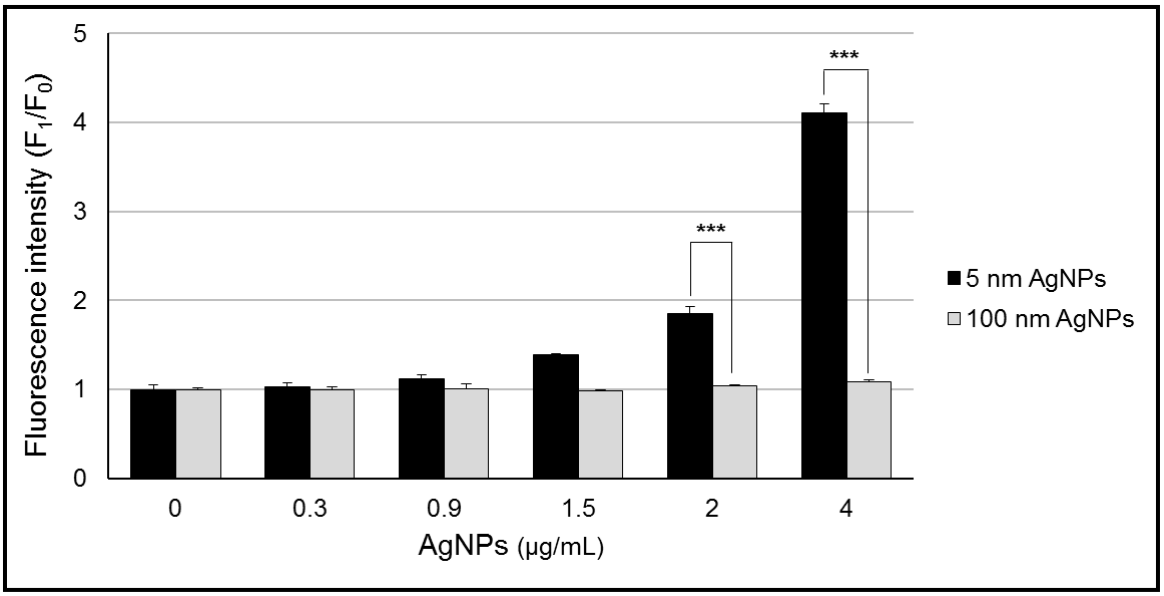

Figure 7. Mitochondrial membrane integrity. RBL2H3 cells were treated with 5 nm and 100 nm AgNPs for 1 hr. JC-1 staining was performed to evaluate disturbances in the mitochondrial membranes. Data represent the mean ± SD. ***p < 0.001.

3.7. Clinical features of skin lesions in AD mice

To investigate the synergistic effect of AgNPs on the induction of AD, ear thickness was measured once a week, and the severity score of the AD-like skin lesions was evaluated once a week. Ear swelling was more severe in mice treated with 4,000 μg/mL 5 nm AgNPs and Ad Biostir (0.78 mm at 3 weeks) than in AD control mice (0.4 mm at 3 weeks) (Fig. 8). In addition, the severity score was higher in mice treated with 4,000 μg/mL 5 nm AgNPs (7 points at 3 weeks) than in AD control mice (2 points at 3 weeks) (Fig. 9).

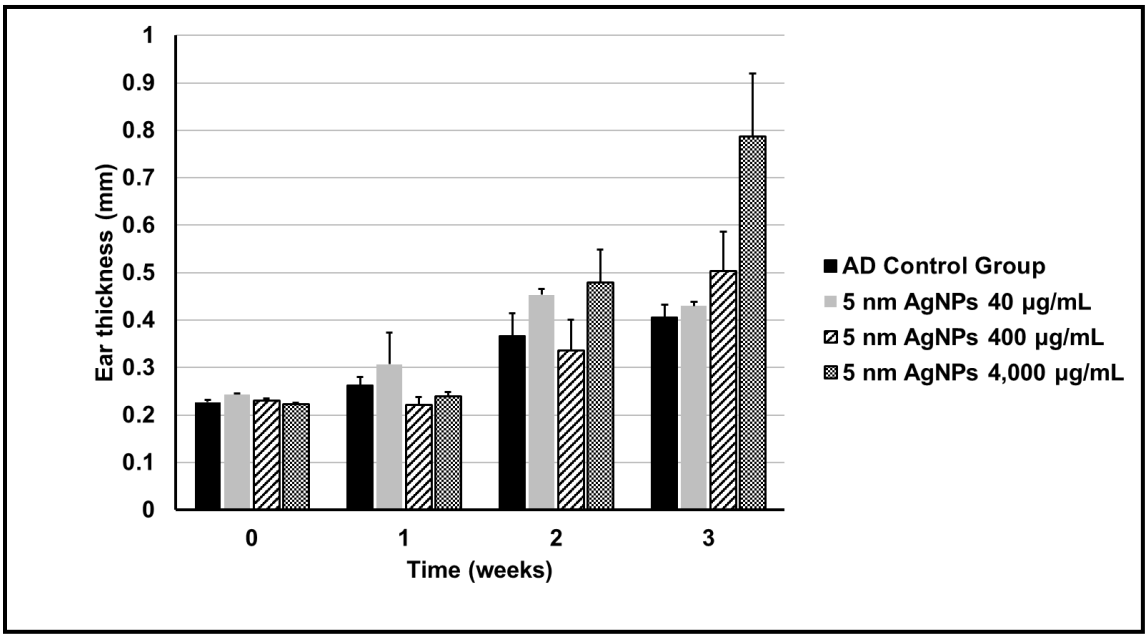

Figure 8. Ear swelling in AD mice. Ear thickness was measured using a dial micrometer. Data represent the mean ± SD. N=3.

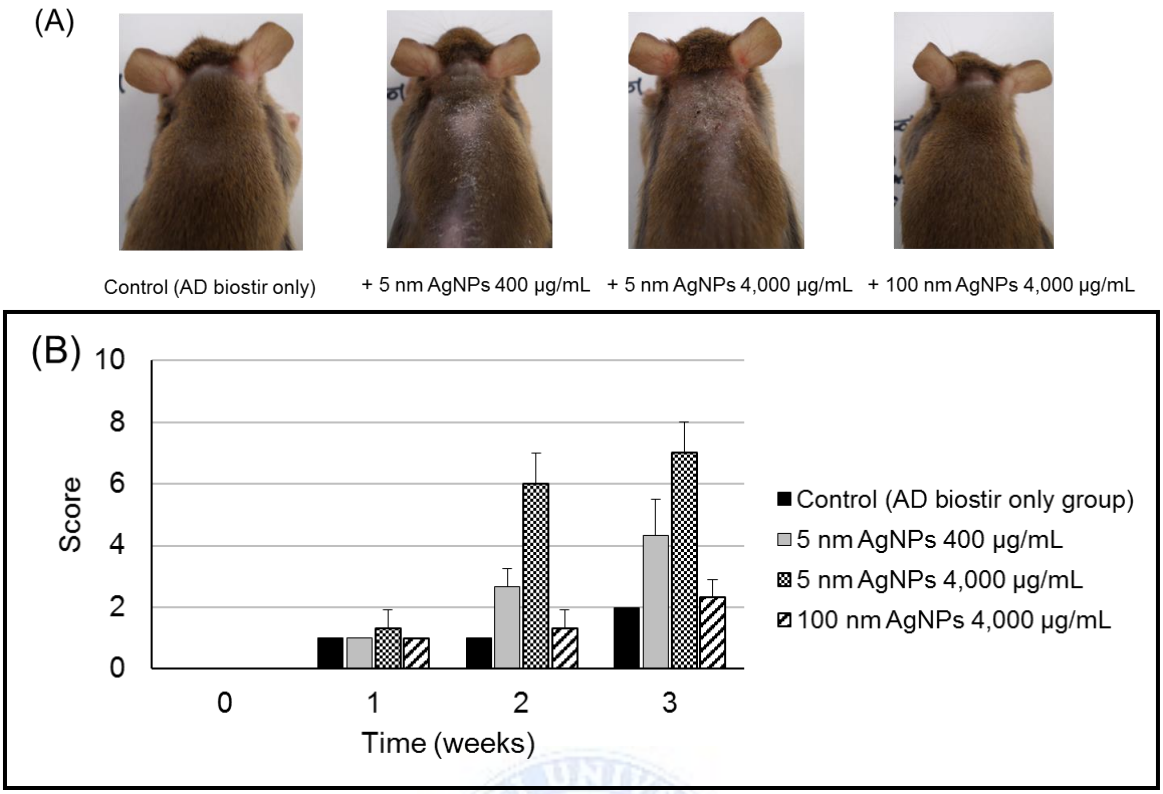

Figure 9. Clinical severity score of skin lesions in AD mice. The score is obtained by grading four signs (erythema/hemorrhage, scaling/dryness, edema, excoriation/erosion), each on a scale of 0 (absent), 1 (mild), 2 (moderate), or 3 (severe). Data represent the mean ± SD. N = 3.

3.8. Histopathological findings in skin lesions of AD mice

Two week samples were used for H&E and toluidine blue staining. The epidermal thickness of the group treated with 5 nm AgNPs + Ad Biostir was thicker (116 ± 14.6 μm) than that of the Ad Biostir-only group (49 ± 9.5 μm) (Fig. 10D). Mast cell numbers in four high-power fields at ×400 magnification were selected randomly and counted. The number of infiltrated mast cells in the skin lesions was higher in the group treated with 5 nm AgNPs + Ad Biostir (23 ± 4.9) than in the Ad Biostir-only group (6 ± 2.3) (Fig. 11D).

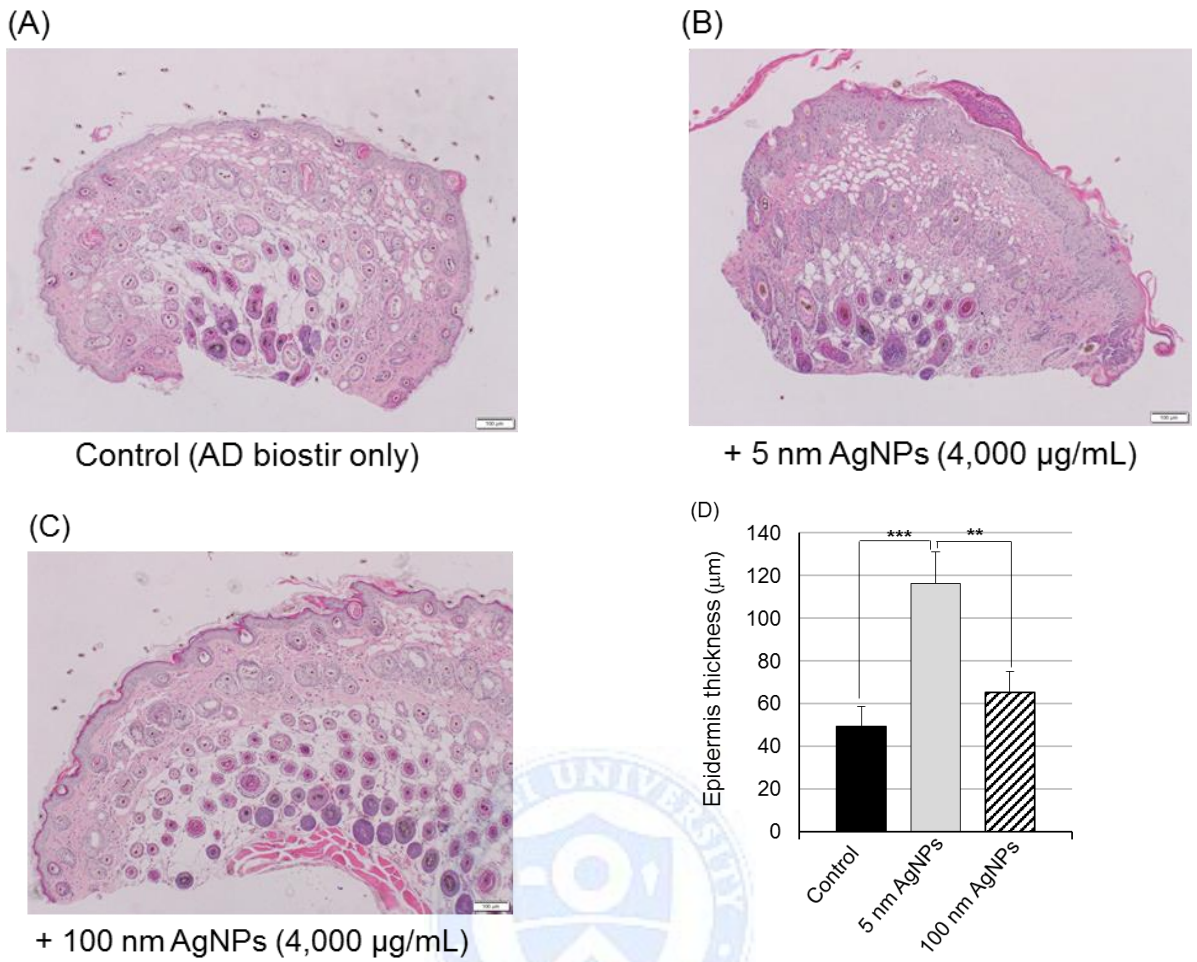

Figure 10. Histological features of the skin lesions in AD mice. (A-C) The dorsal skin was stained with H&E. (D) The epidermis thickness of five regions in each group was measured using a microscope (×100). Data represent the mean ± SD. ***$p < 0.001$, **$p < 0.05$.

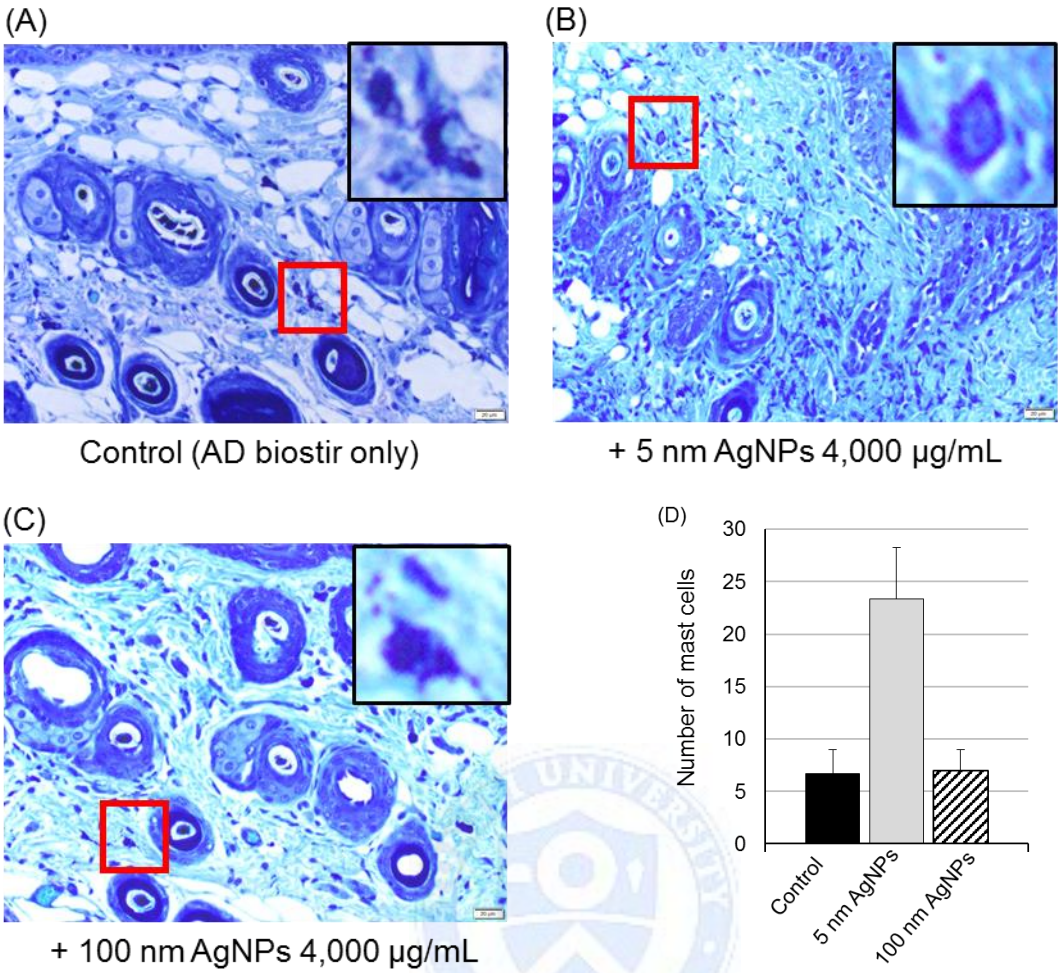

Figure 11. Number of mast cells in the skin lesions of AD mice. (A-C) The dorsal skin was stained with toluidine blue. The number of mast cells/unit area of dermis in four sites chosen at random was counted (×400) (D).

3.9. Total serum IgE levels in AD mice

Total IgE levels in the serum were higher in the group treated with 5 nm AgNPs + Ad Biostir (510 ng/mL at 2 weeks) than in the control group (Fig 12). IgE was not detectable in the control group (Ad Biostir-only group) or the 100 nm AgNPs.

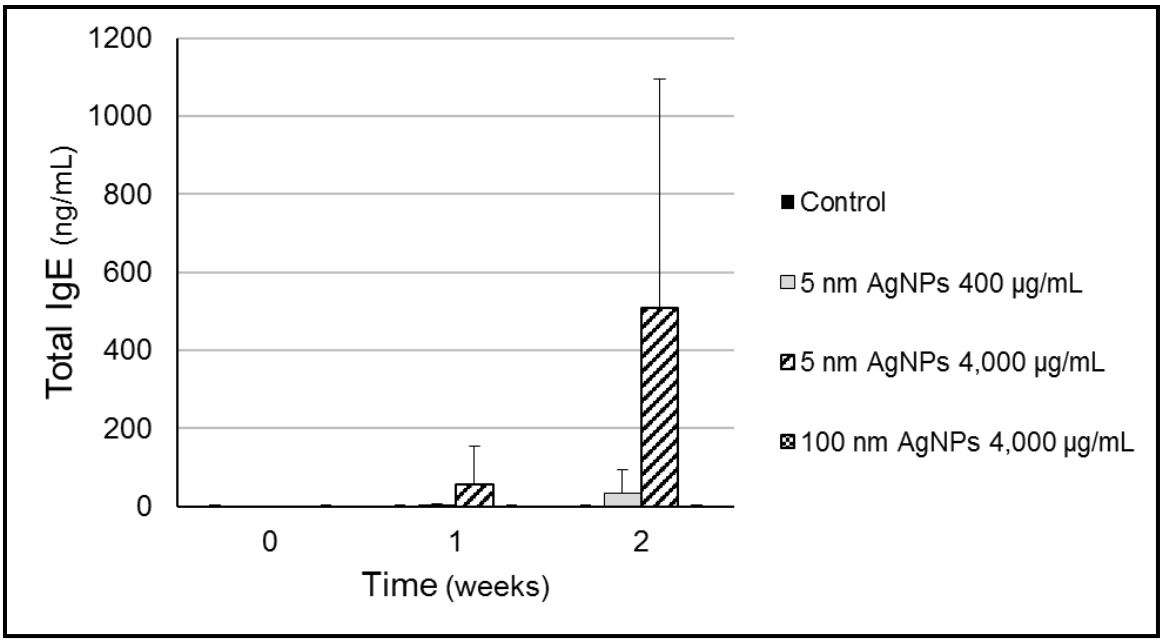

Figure 12. IgE levels in the serum of AD mice. The amount of serum IgE was analyzed using a mouse IgE-specific ELISA Kit. Samples were diluted 1:100 and 1:1,000. Data represent the mean ± SD. N = 3.

4. Discussion

The cardinal pathway of granule release is induced by the attachment of IgE-bound allergens to high-affinity FcεRI receptors on mast cells and the crosslinking of IgE molecules by allergens. These events lead to a complex cascade of intracellular Ca^{2+} signaling (24), which is an essential mechanism for degranulation in mast cells. In this study, it was investigated that whether AgNPs could induce degranulation in mast cells in the absence of IgE crosslinking by allergens. Our data showed that AgNPs induced cytotoxicity and granule release in RBL2H3 mast cells without IgE crosslinking by allergens (Fig. 2 and 3). ROS production was the main toxicity mechanism induced AgNPs (9, 29). Cytotoxicity and granule release were inhibited by the ROS scavenger NAC, indicating that induction of ROS by AgNPs is an important cause of cytotoxicity and granule release. Ca^{2+} influx, the main upstream event in degranulation, was induced in RBL2H3 cells treated with 5 nm AgNPs in buffer with or without Ca^{2+} (Fig. 4). These results indicated that Ca^{2+} influx depended on intracellular Ca^{2+} stores. A recent report has shown that TiO_2 nanoparticles can induce calcium influx in mast cells via an ER-dependent IP3-IP3 receptor pathway (25). Calcium influx was induced by silica nanoparticles in monocytes (26). In addition, Ca^{2+} influx induced by TiO_2 and silica nanoparticles is associated with intracellular Ca^{2+} and granule release.

The ER is the main source of intracellular Ca^{2+} (27). To confirm that the ER was the source of the intracellular Ca^{2+} stores, we used thapsigargin, a known inhibitor of the ER calcium ATPase. Granule release in RBL2H3 cells treated with 5 nm AgNPs was inhibited by thapsigargin (Fig. 5). This result indicated that AgNPs activated the

ER calcium ATPase to induce intracellular Ca^{2+} influx and granule release in RBL2H3 cells.

ROS are chemically reactive molecules that contain oxygen. ROS are produced intracellularly via multiple mechanisms depending on the cell and tissue type. The major sources of ROS are the NADPH oxidase complexes in the cell membrane, ER, peroxisomes, and mitochondria (28). AgNPs reduce the ATP content, causing damage to mitochondria and increasing the production of ROS in a dose-dependent manner. (29). A recent report has shown that calcium release is related to mitochondrial disruption and ROS (30). In this study, hydrogen peroxide and mitochondrial superoxide were induced in RBL2H3 cell treated with 5 nm AgNPs (Fig. 6). Mitochondrial damage was induced in RBL2H3 cells treated with 5 nm AgNPs (Fig. 7). These results suggest that hydrogen peroxide and mitochondrial superoxide induced mitochondrial damage mitochondrial damage, which would cause ER stress and Ca^{2+} influx.

This study demonstrated that 5 nm AgNPs induced granule release in RBL2H3 cells without the crosslinking of IgE molecules. Ca^{2+} influx via the ER and ROS production by the mitochondria were the main cause. Granule release, Ca2+ influx, and ROS production were not observed after treatment with 100 nm AgNPs.

In this study, the effect of AgNPs on AD was examined using NC/Nga mice. Research related to dermal AgNP exposure is mainly restricted to determining the efficacy of wound dressings (31, 32). However, with dermal exposure, it is possible that AgNPs induce immunostimulatory effects. Immunostimulatory effects induced by AgNPs depend on the skin being damaged (33). A recent report showed that 10 nm AgNPs did not induce severe toxic effects in rats up to 2,000 mg/kg (34). However,

our results showed that AgNPs induced immunostimulatory effects in NC/Nga mice. Ear swelling was induced in NC/Nga mice treated with 5 nm AgNPs (Fig. 8). Ear swelling is one of the major inflammatory responses. The response was induced by AgNPs in a dose-dependent manner. Mice treated with 5 nm AgNPs had a high score after 2 weeks (Fig. 9). Some wounds in these mice were a result of scratching behavior. A main feature of AD is dry itchy skin. Intense pruritus and the resulting scratching cause continuous mechanical skin injury that leads to cytokine and chemokine release in the skin. This leads to a further increase in skin permeability that promotes the entry of allergens in the skin (35). Scratching behavior of normally occurs at 6-8 weeks in NC/Nga mice induced with the house dust mite (HDM). It is the first sign of skin changes. Scratching behavior is followed by rapidly developing erythematous, erosive lesions with edema and hemorrhage on the skin (21). Our results indicated that the immunostimulatory effects induced by AgNPs could rapidly lead to atopic symptoms in NC/Nga mice. Furthermore, the histological features of the skin lesions also confirmed AD. The epidermis was thicker in the skin lesions of mice exposed to 5 nm AgNPs (Fig. 10). This indicates that inflammation occurs in lesions treated with AgNPs. Infiltration of mononuclear cells was observed the skin lesions of mice treated with 5 nm AgNPs. Mast cell numbers increased when mice were treated with 5 nm AgNPs. (Fig. 11). The histological features of mice treated with 5 nm AgNPs were consistent with atopic symptoms.

Pathologically, AD is associated with an IgE- mediated hypersensitivity reaction. In this study, the total serum IgE level increased in NC/Nga mice treated with 5 nm AgNPs (Fig. 12). Humans with AD have high levels of IgE antibodies to HDM and

other allergens. High levels of IgE can lead to improvements in AD The pathological features of mice treated with 5 nm AgNPs were consistent with atopic symptoms.

In conclusion, this study showed that AgNPs could aggravate skin symptoms at the early stages of AD in NC/Nga mice. AgNPs induced immunostimulatory effects, such as activation of mast cells via mitochondrial ROS. I suggest that these immunostimulatory effects contribute the development of AD. In recent years, nanotoxicity has been widely studied. However, the research related to direct pathogenic diseases such as AD is insufficient. Our results demonstrate that AgNPs have a synergistic effect on diseases such as AD. Inflammatory effect should be considered and evaluated along with cytotoxicity when studying the effects of AgNP exposure on human physiology.

II. Effects of silver nanoparticles in macrophages

1. Introduction

The dramatic increase in human exposure to nanomaterials has raised concerns regarding their potentially harmful effects on cells (36). From entry sites, such as the skin or respiratory tract, nanoparticles can translocate to other parts of the body (37, 38). Macrophages are active phagocytic cells present in many tissues as resident macrophages, such as alveolar macrophages in the lungs or skin macrophages. The internalization of nanoparticles by phagocytic cells can occur through phagocytosis/macropinocytosis, receptor-mediated endocytosis and passive penetration (39, 40). Phagocytosis and macropinocytosis are mediated by actin polymerization, which causes cell membrane ruffling. The processes inhibited by cytochalasin D (41). Endocytosis can occur as clathrin-dependent endocytosis and caveolae-dependent endocytosis (42). Clathrin-dependent endocytosis is inhibited by chlorpromazine, a cationic amphiphilic drug that prevents the recycling of clathrin (43). Caveolae-dependent endocytosis is inhibited by nystatin (44), an antibiotic and sterol-binding agent that removes membrane cholesterol, which is important for maintaining and sealing the plasma membranes of caveolae (45).

This study was conducted to determine which internalization mechanisms are important for cellular uptake and cellular activation following exposure of macrophages to 5 nm AgNPs. Macrophages were treated with AgNPs at a concentration that does not induce cell death, and IL-8 production was examined. The

results improve our understanding of the effect of AgNPs on macrophages during the induction of immune responses and inflammation.

2. Materials and Methods

2.1. Chemicals

The AgNPs were used the 5 nm AgNPs described on page 4. For cell culture, AgNPs were prepared in RPMI 1640 medium with 2 mM L-glutamine, 10% FBS, and penicillin and streptomycin (100 U/mL each). U937 cells were treated for 1 hr with chlorpromazine (C8183; Sigma, St. Louis, MO, USA.), cytochalasin D (C8273; Sigma), or nystatin (N6261; Sigma) at the indicated concentrations before the addition of nanoparticles. At the concentrations used in this study, the inhibitors were not toxic to U937 cells.

2.2. Cell culture and cytotoxicity assay

The human macrophage cell line U937 was cultured in RPMI 1640 containing 10% FBS and streptomycin and penicillin (100 U/mL each) at 37℃ in a humidified 5% CO_2 incubator. Polymyxin B (InvivoGen, San Diego, CA, USA) was added as described at page 4. Cell viability was assessed using CCK-8 as described on page 5.

2.3. ELISA

To assess the IL-8 concentration in the cell culture supernatants, an enzyme-linked immunosorbent assay (ELISA) was performed using human cytokine IL-8 assay kits (BD Biosciences, San Jose, CA, USA.). The optical densities were measured with a microplate reader at 450 nm.

2.4. Real-time RT-PCR

cDNA was synthesized from total RNA via reverse transcription with oligo-dT primers (Invitrogen). Primer pairs designed to amplify the cDNA encoding IL-8 were prepared using the Universal Probe Library Assay Design Center (Roche Applied Science, Indianapolis, IN, USA.). The primer sequences for IL-8 were as follows: forward, 5'-GTG CAG TTT TGC CAA GGA GT-3' and reverse, 5'-CTC TGC ACC CAG TTT TCC TT-3'. PCR reactions were performed using FastStart DNA Master SYBR Green I reagents and 3 mM $MgCl_2$ according to the manufacturer's instructions (Roche Applied Science) with a 7500 Real-Time PCR system (Applied Biosystems, Foster City, CA, USA.). The PCR cycle parameters were: 2 min at 50℃, 10 min at 95℃ and 40 cycles of 95℃ for 10 sec and 59℃ for 1 min. Real-time RT-PCR data for each gene product was normalized to the levels of glyceraldehyde 3-phosphate dehydrogenase. All transcript levels were reported as the mean ± SD relative to untreated controls from triplicate analyses. One-way analysis of variance was used to assess the differences between the control and experimental groups.

3. Results

3.1. Cytotoxicity in macrophages

The viability of U937 cells declined abruptly when the cells were treated with 5 nm AgNPs 0 -0.8 μg/mL (Fig. 13A). The LC_{50} for the 5 nm AgNPs was 0.36 μg/mL in U937 cells. Next, the effects of inhibiting the endocytosis and phagocytosis of AgNPs was evaluated. After treatment of U937 cells with 0.5 μg/mL AgNPs, neither chlorpromazine, cytochalasin D, nor nystatin prevented cell death (Fig. 13B).

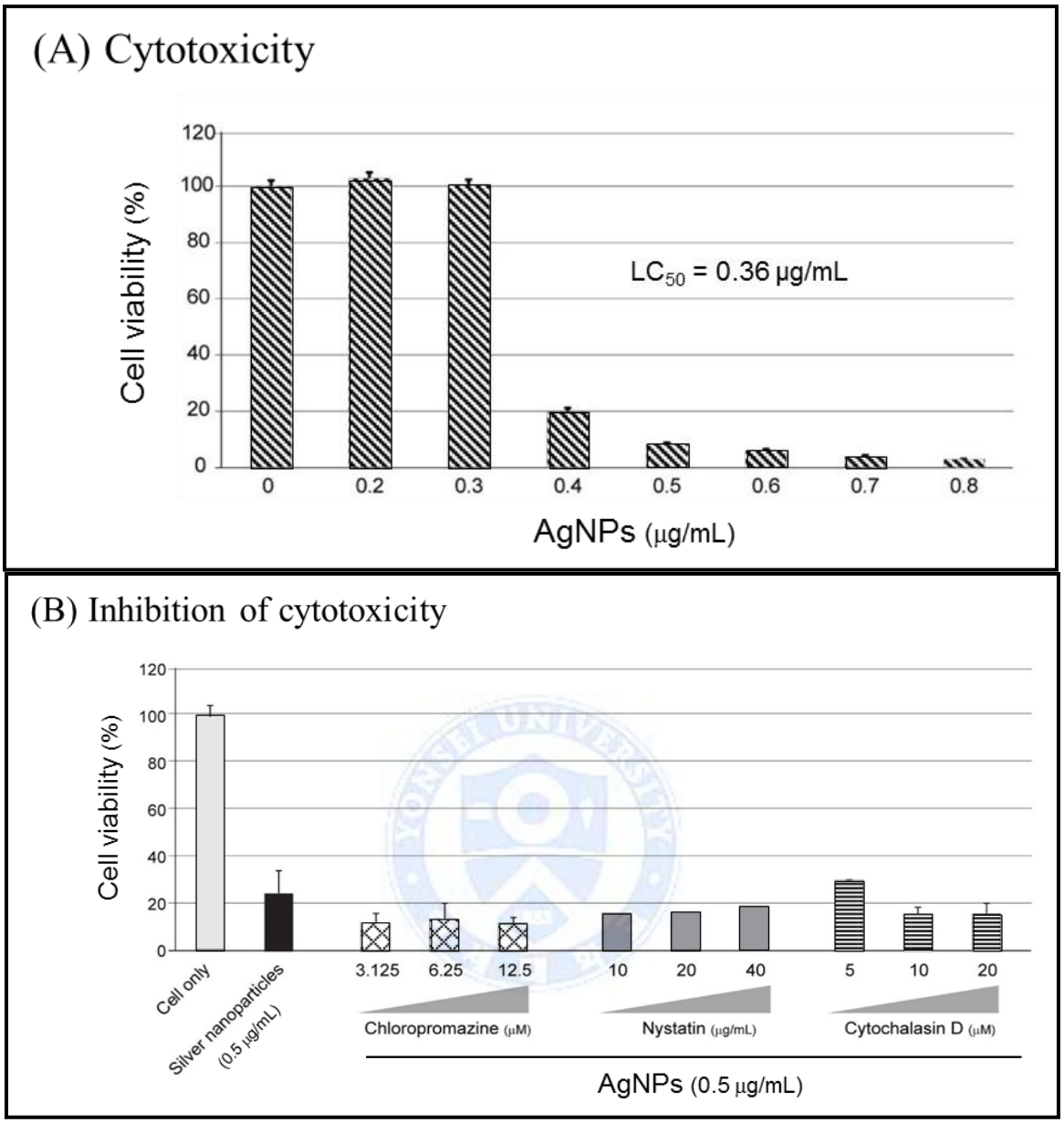

Figure 13. Cytotoxicity of AgNPs in macrophages. (A) Cytotoxicity in U937 cells was assessed with the CCK-8 assay. The LC_{50} of 5 nm AgNPs was 0.36 μg/mL. (B) Each inhibitor was added 1 hr before exposure of the cell to 0.5 μg/mL of 5 nm AgNPs.

3.2. IL-8 production and the effect of endocytosis/phagocytosis inhibitors

As shown in Fig. 14A, relatively high concentrations of chlorpromazine, cytochalasin D and nystatin partially inhibited the production of IL-8 by macrophages after exposure to AgNPs. These findings were confirmed in real-time RT-PCR assay (Fig. 14B).

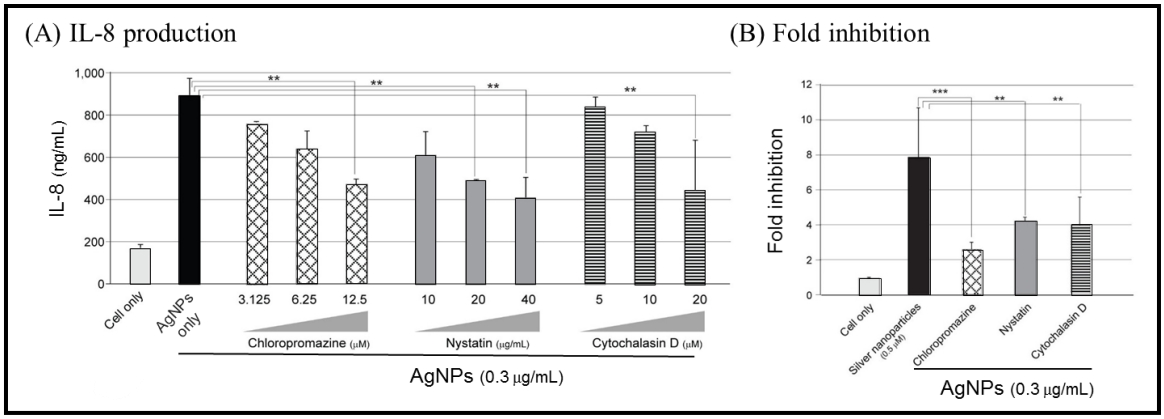

Figure 14. Effects of endocytosis/phagocytosis inhibitors on IL-8 production in macrophages. Chlorpromazine (12.5 μM), nystatin (40 μg/mL), and cytochalasin D (20 μM) were added 1 hr before treatment of the cells with AgNPs. (A) IL-8 levels in the culture supernatants were assessed with ELISA 18 hr after treatment with 5 nm AgNPs. (B) Total RNA was prepared, and real-time RT-PCR was performed.

*$p < 0.05$, †$p < 0.001$.

4. Discussion

The results of this study suggest that a large portion of the 5 nm AgNPs enters the cell by means other than endocytosis and phagocytosis. One mechanism of entry might be direct penetration of the cell membrane, given the extremely small size of the nanoparticles. Quantum dots (46, 47) can penetrate cell membranes as can gold nanoparticles (48, 49). Gold nanoparticles of 2.4 nm in diameter were found to localize in the nucleus via direct penetration, whereas gold nanoparticles 16 nm and larger did not enter the cells (49). Therefore, in addition to entering via endocytosis 5 nm AgNPs might enter cells by penetrating the lipid bilayer in a passive manner.

Tissue macrophages are distributed throughout the body. They secrete a large pool of cytokines when they encounter foreign materials. Among the cytokines that participate in innate immunity, IL-8 recruits neutrophils to acute inflammation sites. A previous study demonstrated that AgNPs triggered macrophages to release IL-8 (9). Therefore, we chose IL-8 as an early responsive indicator for determining when macrophages are exposed to AgNPs.

In this study, a complex mechanism, rather than a dominant mechanism, was found to be involved in the cellular uptake of nanoparticles and the production of IL-8 by macrophages following exposure to AgNPs. The internalizing of nanoparticles has multiple steps. The uptake of quantum dots is dependent on environmental temperatures (50), indicating that a dynamic cellular process is involved. Additionally, the cellular uptake of quantum dots is dependent on the cell type and cell differentiation stage, as demonstrated in dendritic cells. Mature dendritic cells stimulated with lipopolysaccharide exhibited increased uptake of quantum dots when

compared with unstimulated dendritic cells (51). Our real-time RT-PCR data indicated that chlorpromazine inhibited IL-8 production by macrophages treated with nanoparticles to a greater extent than did cytochalasin D or nystatin. Therefore, the role of the clathrin-dependent endocytosis of nanoparticles in for IL-8 production by macrophages might be greater than of caveolin-mediated endocytosis and phagocytosis.

In summary, these results demonstrate that multiple mechanisms, including endocytosis and phagocytosis, contribute to IL-8 production in macrophages following exposure to 5 nm AgNPs. However, endocytosis or phagocytosis inhibitors were did not inhibit the cytotoxicity triggered by these nanoparticles.

Conclusion & Summary

In this study, The toxic mechanism of AgNPs in macrophages, mast cells and NC/Nga mice was investigated.

1. RBL2H3 mast cell viability was dependent on the particles size. Cell death was induced by 5 nm AgNPs. The viability of cells treated with 5 nm and 100 nm AgNPs differed.

2. Granule release was induced by 5 nm AgNPs in RBL2H3 mast cells. Treatment with N-acetyl-1-cystein (NAC) attenuated cell death and granule release.

3. Ca^{2+} influx was induced by 5nm AgNPs in HBSS with or without Ca^{2+}, but not by 100 nm AgNPs.

4. Thapsigargin inhibited granule release induced by 5 nm AgNPs. At the same dose, 100 nm AgNPs did not induce granule release.

5. The production of hydrogen peroxide and superoxide increased in a dose-dependent in cells treated with 5 nm AgNPs. Hydrogen peroxide and superoxide were not induced by 100 nm AgNPs.

6. Mitochondrial membrane damage was induced by 5 nm AgNPs, but not by 100 nm AgNPs.

7. Mouse ear swelling induced in mice treated with 5 nm AgNPs, as did the severity score.

8. The epidermis of mice treated with 5 nm AgNPs was thicker than that of control mice. The number of infiltrated mast cells in the skin lesions increased. Total serum IgE levels also increased in mice treated with 5 nm AgNPs.

9. Multiple mechanisms, including endocytosis and phagocytosis, contribute to IL-8 production in macrophages following exposure to 5 nm AgNPs.

10. After treatment of U937 cells with 5 nm AgNPs, neither chlorpromazine, cytochalasin D, nor nystatin prevented cell death.

These results show that AgNPs can aggravate skin symptoms at the early stages of AD in NC/Nga mice. AgNPs induced immunostimulatory effects, including the activation of mast cells via mitochondrial ROS. Multiple mechanisms, including endocytosis and phagocytosis, contribute to IL-8 production in macrophages following exposure to 5 nm AgNPs. These immunostimulatory effects might contribute to the development of AD. Thus, inflammatory effects should be considered and evaluated along with cytotoxicity when studying the effects of AgNP exposure on human physiology.

References

Effects of silver nanoparticles in mast cells

1. Jonathan H. Shannahan and Jared M. Brown, Engineered nanomaterial exposure and the risk of allergic disease. Curr Opin Allergy Clin Immunol. 2014;14:95-9.

2. Luan J, Wu J, Zheng Y, Song W, Wang G, Guo J, Ding X. Impregnation of silver sulfadiazine into bacterial cellulose for antimicrobial and biocompatible wound dressing. Biomed Mater. 2012;7:065006.

3. Adam D. McFarland, Richard P. Van Duyne. Single Silver Nanoparticles as Real-Time Optical Sensors with Zeptomole Sensitivity.Nano Letters. 2003;3:1057-1062.

4. Tian Xia, Ning Li, Andre E. Nel. Potential Health Impact of Nanoparticles. Annu Rev Public Health. 2009;30:137-50.

5. Yang E-J, Jang J, Kim S, Choi I-H. Silver nanoparticles as a smart antimicrobial agent. J Bacteriol Virol. 2012;42:177-9.

6. Toki S, Omary RA, Wilson K, Gore JC, Peebles RS Jr, Pham W. A comprehensive analysis of transfection-assisted delivery of iron oxide nanoparticles to dendritic cells. Nanomedicine. 2013;9:1235-44.

7. Kim S, Choi IH. Phagocytosis and endocytosis of silver nanoparticles induce interleukin-8 production in human macrophages. Yonsei Med J. 2012;53:654-7.

8. Eun-Jeong Yang, Seungjae Kim, Jong Soo Kim, In-Hong Choi. Inflammasome formation and IL-1b release by human blood monocytes in response to silver nanoparticles. Biomaterials. 2012;33:6858-6867.

9. Park J, Lim DH, Lim HJ, Kwon T, Choi JS, Jeong S, et al. Size dependent macrophage responses and toxicological effects of Ag nanoparticles. Chem Commun. 2011;47:4382-4.

10. Cavalieri F, Tortora M, Stringaro A, Colone M, Baldassarri L. Nanomedicines for antimicrobial interventions. J Hosp Infect. 2014;88:183-90.

11. Balzar S, Fajt ML, Comhair SA, Erzurum SC, Bleecker E, Busse WW, Castro M, Gaston B, Israel E, Schwartz LB, Curran-Everett D, Moore CG, Wenzel SE. Mast cell phenotype, location and activation in severe asthma. Am J Respir Crit Care Med. 2011;183:299-309.

12. Zhao L et al. A rodent model for allergic dermatitis induced by flea antigens. Vet Immunol Immunopathol. 2006;114:285-296.

13. Gordon JR, Galli SJ. Release of both preformed and newly synthesized tumor necrosis factor alpha (TNF-alpha)/cachectin by mouse mast cells stimulated via the Fc epsilon RI. A mechanism for the sustained action of mast cell-derived TNF-alpha during IgE-dependent biological responses. J Exp Med. 1991;174:103-7.

14. Siraganian RP. Mast cell signal transduction from the high-affinity IgE receptor. Curr Opin Immunol. 2003;15:639-46.

15. T. Terui, Analysis of the mechanism for the development of allergic skin inflammation and the application for its treatment: overview of the pathophysiology of atopic dermatitis. J Pharmacol Sci. 2009;110:232-6.

16. Trautmann A, Akdis M, Kleemann D, Altznauer F, Simon HU, Graeve T. T cell-mediated Fas-induced keratinocyte apoptosis plays a key pathogenetic role in eczematous dermatitis. J Clin Invest. 2000;106:25–35.

17. Pastore S, FanalesBelasio E, Albanesi C, Chinni LM, Giannetti A, Girolomoni G. Granulocyte macrophage colony-stimulating factor is overproduced by keratinocytes in atopic dermatitis - Implications for sustained dendritic cell activation in the skin. J Clin Invest. 1997;99:3009–3017.

18. Novak N, Bieber T, Leung DY. Immune mechanisms leading to atopic dermatitis. J Allergy Clin Immunol. 2003;112:S128–139.

19. Leung DYM, Boguniewicz M, Howell MD, Nomura I, Hamid OA. New insights into atopic dermatitis. J Clin Invest. 2004;113:651–657.

20. Liu FT, Goodarzi H, Chen HY. IgE, mast cells and eosinophils in atopic dermatitis. Clin Rev Allergy Immunol. 2011;41:298-310.

21. Takaoka A, Arai I, Sugimoto M, Honma Y, Futaki N, Nakamura A, Nakaike S. Involvement of IL-31 on scratching behavior in NC/Nga mice with atopic-like dermatitis. Exp Dermatol. 2006;15:161-7.

22. Kondo, K., Nagami, T. and Tadokoro, S. Differences in haematopoeitic death among inbred strains of mice. In Comparative cellular and species radiosensitivity. Igakushoin. 1969;20.

23. Yamamoto M, Haruna T, Yasui K, Takahashi H, Iduhara M, Takaki S, Deguchi M, Arimura A. Allergol Int. 2007;56:139-48.

24. Gilfillan AM, Tkaczyk C. Integrated signalling pathways for mast-cell activation. Nat Rev Immunol. 2006;6:218-30.

25. Chen EY, Garnica M, Wang YC, Mintz AJ, Chen CS, Chin WC. A mixture of anatase and rutile TiO_2 nanoparticles induces histamine secretion in mast cells. Part Fibre Toxicol. 2012;9:2.

26. Kim S, Jang J, Kim H, Choi H, Lee K, Choi IH. The effects of silica nanoparticles in macrophage cells. Immune Netw. 2012;12:296-300.

27. Feske S, Wulff H, Skolnik EY. Ion channels in innate and adaptive immunity. Annu Rev Immunol. 2015;33:291-353.

28. D Han, E Williams, E Cadenas. Mitochondrial respiratory chain-dependent generation of superoxide anion and its release into the intermembrane space. Biochem J. 2001;353:411–416.

29. AshaRani PV, Low Kah Mun G, Hande MP, Valiyaveettil S. Cytotoxicity and genotoxicity of silver nanoparticles in human cells. ACS Nano. 2009;3:279-90.

30. Zhang K, Kaufman RJ. From endoplasmic-reticulum stress to the inflammatory response. Nature. 2008;454:455-62.

31. Tian J, Wong KK, Ho CM, Lok CN, Yu WY, Che CM, Chiu JF, Tam PK. Topical delivery of silver nanoparticles promotes wound healing. ChemMedChem. 2007;2:129-36.

32. Archana D, Singh BK, Dutta J, Dutta PK. Chitosan-PVP-nano silver oxide wound dressing: In vitro and in vivo evaluation. Int J Biol Macromol. 2015;73:49-57.

33. Johnston HJ, Hutchison G, Christensen FM, Peters S, Hankin S, Stone V. A review of the in vivo and in vitro toxicity of silver and gold particulates: particle attributes and biological mechanisms responsible for the observed toxicity. Crit Rev Toxicol. 2010;40:328-46.

34 Kim JS, Song KS, Sung JH, Ryu HR, Choi BG, Cho HS, Lee JK, Yu IJ. Genotoxicity, acute oral and dermal toxicity, eye and dermal irritation and corrosion and skin sensitisation evaluation of silver nanoparticles. Nanotoxicology. 2013;7:953-60.

35. Homey B, Steinhoff M, Ruzicka T, Leung DY. Cytokines and chemokines orchestrate atopic skin inflammation. J Allergy Clin Immunol. 2006;118:178–189.

The effects of silver nanoparticles in macrophages

36. Yokel RA, Macphail RC. Engineered nanomaterials: exposures, hazards and risk prevention. J Occup Med Toxicol. 2011;6:7.

37. Hackenberg S, Scherzed A, Kessler M, Hummel S, Technau A, Froelich K, et al. Silver nanoparticles: evaluation of DNA damage, toxicity and functional impairment in human mesenchymal stem cells. Toxicol Lett. 2011;201:27-33.

38. Jang J, Lim DH, Choi IH. The impact of nanomaterials in immune system. Immune Netw. 2010;10:85-91.

39. Tantra R, Knight A. Cellular uptake and intracellular fate of engineered nanoparticles: a review on the application of imaging techniques. Nanotoxicology. 2011;5:381-92.

40. Zhao F, Zhao Y, Liu Y, Chang X, Chen C, Zhao Y. Cellular uptake, intracellular trafficking and cytotoxicity of nanomaterials. Small. 2011:7;1322-37.

41. Kerr MC, Teasdale RD. Defining macropinocytosis. Traffic. 2009;10:364-71.

42. Kumari S, Mg S, Mayor S. Endocytosis unplugged: multiple ways to enter the cell. Cell Res. 2010;20:256-75.

43. Hernaez B, Alonso C. Dynamin- and clathrin-dependent endocytosis in African swine fever virus entry. J Virol. 2010;84:2100-9.

44. Santibanez JF, Blanco FJ, Garrido-Martin EM, Sanz-Rodriguez F, del Pozo MA, Bernabeu C. Caveolin-1 interacts and cooperates with the transforming growth factor-beta type I receptor ALK1 in endothelial caveolae. Cardiovasc Res. 2008;77:791-9.

45. Greulich C, Diendorf J, Simon T, Eggeler G, Epple M, Köller M. Uptake and intracellular distribution of silver nanoparticles in human mesenchymal stem cells. Acta Biomater. 2011;7:347-54.

46. Wang T, Bai J, Jiang X, Nienhaus GU. Cellular uptake of nanoparticles by membrane penetration: a study combining confocal microscopy with FTIR spectroelectrochemistry. ACS Nano. 2012;6:1251-9.

47. Dubavik A, Sezgin E, Lesnyak V, Gaponik N, Schwille P, Eychmüller A. Penetration of amphiphilic quantum dots through model and cellular plasma membranes. ACS Nano. 2012;6:2150-6.

48. Lin J, Zhang H, Chen Z, Zheng Y. Penetration of lipid membranes by gold nanoparticles: insights into cellular uptake, cytotoxicity and their relationship. ACS Nano. 2010;4:5421-9.

49. Oh E, Delehanty JB, Sapsford KE, Susumu K, Goswami R, BlancoCanosa JB, et al. Cellular uptake and fate of PEGylated gold nanoparticles is dependent on both cell-penetration peptides and particle size. ACS Nano. 2011;5:6434-48.

50. Zhang A, Guan Y, Xu LX. Theoretical study on temperature dependence of cellular uptake of QDs nanoparticles. J Biomech Eng. 2011;133:124502.

51. Zhang LW, Bäumer W, Monteiro-Riviere NA. Cellular uptake mechanisms and toxicity of quantum dots in dendritic cells. Nanomedicine (Lond). 2011;6:777-91.

ABSTRACT (IN KOREAN)

은나노입자의 면역세포 자극 효과와 아토피 동물 모델에서 아토피 항진 효과

김 승 재

연세대학교 대학원 나노메디컬 협동과정

(지도교수 최 인 홍)

제조 나노물질이 다양한 산업 분야에서 이용되면서 인체는 직·간접적으로 나노물질에 노출되고 있다. 본 연구에서는 나노물질의 면역계에 대한 영향을 파악하고자 대표적인 제조 나노물질인 은나노입자를 이용하여 비만세포와 대식세포 그리고 아토피 동물 모델을 이용한 연구를 수행하였다.

첫째, 비만세포는 아토피 및 천식 등 알레르기 반응에서 중요한 면역세포이다. 5 nm 또는 100 nm 은나노입자가 비만세포(RBL2H3)를 활성화시키는지 관찰하기 위하여 세포독성을 유발하지 않는 낮은 농도의 5 nm 은나노입자를 처리하면 비만세포에서 세포 내 칼슘이온이 증가하고, 탈과립 현상이 유도되며, 더불어 미토콘드리아막 손상과 활성산소 생성이 유도되었다. 그러나 100 nm 은나노입자는 동일한 농도에서 이러한 현상을 유발하지 않았다.

둘째, 아토피 동물 모델 마우스(NC/Nga)에서 은나노입자에 의한 아토피 항진 작용을 확인하기 위해 집먼지진드기 연고와 은나노입자를 동시에 피부에 발라주었다. 귓볼 두께 및 피부 임상 증상을 측정한 결과 5 nm 은나노입자를 투여한 군에서 귀의 부종이 더 증가하였고, 피부 임상 증상도 증가하였다. 조직학적 소견을 통하여 5 nm 은나노입자를 투여한 군에서는 표피가 두꺼워지고 진피 내 비만세포의 수가 증가함을 관찰하였고, 혈액 총 IgE 양이 증가함을 관찰하였다. 100 nm 은나노입자를 투여한 군에서는 이러한 효과가 관찰되지 않았다. 이를 통하여 5 nm 은나노입자가 아토피 동물 모델에서 아토피 증상을 다소 빨리 유도하며 증상도 악화시킴을 확인하였다.

셋째, 대식세포는 선천면역계 세포로서 탐식작용을 통하여 미생물을 제거하고 염증 cytokine 을 생성하여 선천연역을 항진시킬 뿐 아니라 항원을 T 림프구로 전달하고, 적응면역을 조절하는 cytokine 을 생성한다. 대식세포(U937)에 5 nm 은나노입자를 투여하면 IL-8 생성이 유도되는데 이는 은나노입자의 탐식 및 세포 내 이입에 의하여 매개됨을 확인하였다.

본 연구를 통하여 은나노입자는 세포독성을 유발하지 않는 낮은 농도에서 면역세포의 기능을 활성화시키고, 아토피 질환을 악화시켰으며 이 효과는 은나노입자의 크기가 작을수록 더욱 높아짐을 파악하였다. 이러한 결과는 나노물질의 면역 독성 또는 면역계 활성화의 기전을 이해하고, 유해성 평가법 개발에 필요한 정보를 제공할 수 있을 것으로 기대한다.

핵심어 : 은나노입자, 비반세포, 대식세포, 아토피 동물 모델, 활성산소, 싸이토카인.

Publication list

1. The effects of silica nanoparticles in macrophage cells. Kim S, Jang J, Kim H, Choi H, Lee K, Choi IH. Immune Netw. 2012:12;296-300.

2. Phagocytosis and endocytosis of silver nanoparticles induce interleukin-8 production in human macrophages. Kim S, Choi IH. Yonsei Med J. 2012:53;654-7.

3. Inflammasome formation and IL-1β release by human blood monocytes in response to silver nanoparticles. Yang EJ, Kim S, Kim JS, Choi IH. Biomaterials. 2012:33;6858-67.

4. The effects of sub-lethal concentrations of silver nanoparticles on inflammatory and stress genes in human macrophages using cDNA microarray analysis. Lim DH, Jang J, Kim S, Kang T, Lee K, Choi IH. Biomaterials. 2012:33;4690-9.

5. Silver nanoparticles as a smart antimicrobial agent. Eun-Jeong Yang, Jiyoung Jang, Seungjae Kim and In-Hong Choi. Journal of Bacteriology and Virology 2012:42;177-179.